EFFECT OF Er ADDITION AND SOLUTION TREATMENT ON THE MICROSTRUCTURE AND MECHANICAL PROPERTIES OF HYPOEUTECTIC Al–10%Mg_2Si–3.5%Cu ALLOY

Xiaofeng Wu
School of Mechanical and Vehicle Engineering, Nanchang Institute of Technology, Nanchang 330108, People's Republic of China

Fufa Wu and Rongda Zhao
School of Materials Science and Engineering, Liaoning University of Technology, Jinzhou 121001, People's Republic of China

https://doi.org/10.1007/s40962-024-01346-0

Abstract

The effects of Er addition and solution treatment on the microstructure characteristics, tensile properties, and fracture behavior of a hypoeutectic Al–10%Mg_2Si–3.5%Cu alloy were systematically studied. The results showed that the addition of 0.45 wt% Er to hypoeutectic Al–10Mg_2Si alloy without and with the addition of 3.5 wt% Cu can significantly reduce the grain sizes of the eutectic Mg_2Si phase and α-Al/Mg_2Si eutectic cell, and transform the morphology of the eutectic Mg_2Si from coarse Chinese characters to thin stripes, dots, and fibers. The modification of eutectic Mg_2Si is attributed to the inhibition of Er on the heterogeneous nucleation of AlP by forming Er, P-containing phases, and the enrichment of Er atoms around eutectic Mg_2Si, which inhibits the growth of eutectic Mg_2Si and promotes a change in its growth direction. The solid solution treatment causes the eutectic Mg_2Si to tend towards spheroidization, which is promoted by the addition of Er. The addition of 0.45 wt% Er simultaneously improves the strength and plasticity of the cast alloys without and with the addition of 3.5 wt% Cu. The solid solution treatment further improved the tensile properties of the studied alloys. The improvement in strength of the alloy after as-cast and T6 treatment is due to the obstruction of fine eutectic Mg_2Si and containing-Er/Cu intermetallic compound particles on dislocations, while the improvement of plasticity mainly lies in the reduction of stress concentration and stress uniformity around eutectic Mg_2Si and intermetallic compounds caused by the regularity and spheroidization of their morphology.

Keywords: *Al–Mg_2Si–Cu alloy, Er, solution treatment, eutectic Mg_2Si, tensile property*

Introduction

Hypoeutectic Al–Si–Mg alloys are currently the most widely used cast aluminum alloy. The eutectic Si in the alloys is used as the second phase reinforcing Al matrix. But when the weight ratio of Mg to Si reaches 1.73, the intermetallic compound Mg_2Si will precipitate during the solidification process of the alloys, completely replacing the Si phase[1] and this type of Al–Si–Mg alloy is also known as Al-Mg_2Si alloy.[1–3] In recent years, with the development of the automotive and aerospace industries, there has been an increasing demand for lightweight components that can reduce energy consumption and air pollution. Therefore, the Al–Mg_2Si alloys reinforced by the Mg_2Si which precipitated in the cast state as second phase have attracted attention due to their advantages of low density, high specific strength, high specific stiffness, and dimensional stability, compared to the Al–Si–Mg alloys reinforced by Si phase.[2] In the Al–Mg_2Si alloys, Al and Mg_2Si can form a pseudo-eutectic system. From the pseudo-binary Al–Mg_2Si phase diagram,[3] it can be seen that the content of Mg_2Si phase in the eutectic point of this series of alloys is 13.9 wt%. Therefore, the alloys with Mg_2Si content less than 13.9 wt% are hypoeutectic

Xiaofeng Wu and Fufa Wu have equally contributed to this work as first author.

Received: 29 January 2024 / Accepted: 03 April 2024
Published online: 12 May 2024

components. Hypoeutectic Al–Mg_2Si alloys such as Al–10%Mg_2Si alloy have high comprehensive mechanical properties and are suitable for making structural components that can withstand large loads in automobiles. Unfortunately, however, the eutectic Mg_2Si in hypoeutectic Al–Mg_2Si alloys, formed under normal solidification conditions, present coarse Chinese character-like and plate-like morphology, seriously deteriorating the mechanical properties of the alloys, especially their plasticity and toughness.[4]

In order to refine the coarse eutectic Mg_2Si and improve mechanical properties of the Al–Mg_2Si alloys, some trace elements or compounds such as Bi,[4] Sr,[5] TiB_2,[6] and Sb[7] have been added to the alloy melt and the size of eutectic Mg_2Si particles was refined and their morphology were changed to herringbone, spherical and fibrous, improving the mechanical properties of the alloy to varying degrees.

In recent years, there have been some studies on the modification of eutectic Si phase by rare earth element Er in cast Al–Si alloys. Hu et al.[8] demonstrated that the addition of 0.6 wt% Er can transform the morphology of eutectic Si phase in die-cast ADC12 alloy from coarse plate-like into fine dendritic, effectively improving the mechanical properties of the alloy. Colombo et al.[9] reported that adding 0.22 wt% Er to Al–7%Si–0.4%Mg (A356) alloy causes the fragmentation and spheroidization of eutectic Si precipitated in cast state. Pandee et al. [10] revealed that the reason for Er's modification of eutectic Si in Al–7Si–0.3Mg alloy is due to its strong inhibition of nucleation and alteration of its growth mode.

Alloying is another effective way to improve the mechanical properties of Al alloys. As one of the most commonly used alloying elements, Cu addition in Al alloys significantly enhances the strength of the alloys due to the formation of metastable secondary nano-scaled dispersoids such as Q'' or θ' attained during the age-hardening treatment.[11] However, for Cu-containing Al–Si (Mg_2Si) alloys, especially those with high Cu content ($\geq$3.0%), the coarse block-like and network-like Cu-containing intermetallic compounds precipitated along grain boundaries and phase interfaces in the cast state significantly reduce the elongation of the alloys to 1.2%,[12] and such high brittleness can easily cause cracking of castings and limit the practical applications of these alloys.

The addition of Er also has a significant impact on the Cu-containing phases in aluminum alloys. Li et al.[13] found that the Cu-containing phases precipitated in Al–Cu–Mg–Ag alloy without and with the addition of Er were distributed at grain boundaries, and the precipitated phase in the alloy without the addition of Er was coarse block-like Al_2Cu phase, while that in the alloy with the addition of Er, the Al_2Cu phase was replaced by a fine feathered Al_8Cu_4Er phase. Huang et al.[14] reported that the Cu-containing intermetallics in high-strength Al–Zn–Mg–Cu alloys with the addition of Er included quaternary T (AlZnMgCu), Al_7Cu_2Fe, Mg (Zn, Cu, Al)$_2$, and Al_8Cu_4Er phases. Among them, the Al_8Cu_4Er phase presented a fine granular structure and distributed in the edge of (α-Al+T) non-equilibrium layered eutectic phase.

Research has shown that solid solution treatment not only affects the solid solution of alloy elements and their compounds, but also has a significant impact on the morphology, size, and distribution of eutectic Si or Mg_2Si phases, and mechanical properties of the alloys. Wislei et al.[15] found that after T4 treatment, only a few eutectic Si particles in unmodified Al–9%Si alloy showed spherical shape, while the majority still retained the rod-shaped shape in as cast state, with only a decrease in length. However, in the alloy samples modified by Na and treated by T4, all eutectic Si particles had transformed into spherical shapes. Jin et al. used rare earth Eu elements to modify the Mg_2Si phase in Al–15%Mg_2Si[16] composite, and further improved their morphology through T6 heat treatment. After heat treatment, the eutectic Mg_2Si dissolves and appears as short dots. For hypoeutectic Al–Mg_2Si alloy, Li et al.[17] found that after 6 h of solid solution treatment at 520 °C, the long rod-like eutectic Mg_2Si in Al–10%Mg_2Si alloy transformed into short fiber-like and spherical morphology.

Up to now, there are few detailed studies on the effects of adding Er and solution treatment on the eutectic Mg_2Si, Cu-containing intermetallics in hypoeutectic Al–Mg_2Si casting alloys. Therefore, the purpose of this work is to investigate the synergistic influence of rare earth element Er and solute element on the microstructure characteristics, tensile properties and fracture behavior of a hypoeutectic Al–10%Mg_2Si alloy, and their influence mechanisms have been further analyzed.

Experimental Procedures

Specimen Preparation

Al–10%Mg_2Si alloys without and with Er and/or Cu additions were prepared using industrial pure aluminum ingots (99.7%), pure magnesium ingots (99.65%), Al–5%Cu, Al–5%Er and Al–30%Si master alloys as raw materials. Firstly, a resistance furnace was used to prepare 8 kg of melt in a graphite crucible, and the pure Al ingot, the preheated Al–30%Si, Al–5%Cu and Al–5%Er master alloys were melt into the crucible. During the melting process, the temperature of the furnace was controlled between 740 to 760 °C. After the alloys were melted, the pure magnesium ingot wrapped in aluminum foil was preheated to 200 °C and pressed into the melt with a pressure spoon at 680 °C holding for 10 min, and additional Mg and Er accounting for an extra of 15 wt% of the

Table 1. Chemical compositions of the Experimental Alloys (wt%)

Alloy(wt%)	Si	Mg	Cu	Er	Cr	Mn	Zr	Fe	Ti	Al
0Er+0Cu	3.62	6.47	<0.01	<0.01	<0.01	0.01	<0.01	0.17	<0.01	Bal.
0.45Er+0Cu	3.77	6.28	<0.01	0.46	<0.01	0.01	<0.01	0.20	<0.01	Bal.
0Eru+3.5Cu	3.59	6.39	3.48	<0.01	<0.01	0.02	<0.01	0.19	<0.01	Bal.
0.45Er+3.5Cu	3.58	6.41	3.51	0.45	<0.01	0.03	<0.01	0.16	<0.01	Bal.

target composition to the balance melting losses including oxidation and evaporation losses, etc. Then, the melt was degassed by dry hexachloroethane (C_2Cl_6) degasser (0.5 wt% of the alloy). Subsequently, the samples for composition measurement was taken and the results of chemical composition analysis of ingots by inductively coupled plasma atomic emission spectroscopy (ICP-AES) are listed in Table 1. After the slag was skimmed from the melt, the melt was poured into a naturally cooled permanent steel mould, preheated at 220 ± 5 °C for 30 min, to obtain φ 20 × 120 mm cylindrical test bars for microstructural characterization and cast tensile rods at 740 °C. After casting, a T6 heat treatment was performed on all samples. Solid solution treatment was carried out at 500 °C for 8 h, followed by immediate quenching in water at room temperature, and by artificial aging at 160 °C for 6 h, and then air cooling.

Microstructural Characterization

The metallographic samples were cut from 1/3 of the bottom of the bars, and prepared by using standard mechanical polishing and corrosion in 4 vol% HF alcohol solution for 15 s. After 100–1000*x* photos of the corroded metallographic samples being collected by using Zeiss Leica DM4000 optical microscope (OM), they were imported into the Image Pro Plus 6.0 image analyzer for image analysis, and the average length (L_M) and length to diameter ratio (L/B_M) of eutectic Mg_2Si crystals were measured separately by using the linear intercept method. 20 fields of view were select randomly, 30 data for each phase in each field were measured, and the average of the measurements were taken as the final result. Meanwhile, the intermetallic compounds and compositions of the matrix were further characterized by Zeiss SIGMA 500 field emission scanning electron microscope (FE-SEM) with energy dispersive X-ray (EDX). The phase composition was identified by D/max-2500 diffractometer (XRD) with Cu K_α as the radiation source. In addition, in order to observe the three-dimensional (3D) morphology of the eutectic Mg_2Si phase, the samples were immersed in a concentrated NaOH solution of 20 vol% for 20 min to obtain a deeply corroded samples, which were observed using FE-SEM.

Tensile Testing

The permanent steel mould, the castings+gating system for the cast tensile rod and the dimensions of tensile specimen are shown in Fig. 1. The Al–10%Mg_2Si alloys were subjected to tensile testing in accordance with the ASTM standard. The specimens were cut from the cast tensile rods. On the Zwick/Roell Z100 tensile testing machine controlled by the computer, tensile testing was conducted at a tensile rate of 0.2 mm/min. Six tensile samples were tested for each alloy, and the average values were taken. And the transverse and longitudinal fracture surfaces of the tensile specimen were observed using SEM.

Results

Microstructural Characterization

As-cast Condition

Figure 2 illustrates the XRD diffraction patterns of Al–10%Mg_2Si alloy without and with Er or/and Cu additions. From the figure, it can be seen that the alloy without Er and Cu additions is composed of α-Al and Mg_2Si phases, and no diffraction peaks were detected in the XRD results for other compounds. After adding 0.45 wt% Er, the phase composition of the alloy did not change significantly due to the small amount Er added; in the Al–10%Mg_2Si alloy with 3.5 wt% Cu added separately, Al_2Cu phase and Al–Cu–Mg–Si quaternary phase appeared except for the α-Al and Mg_2Si phases. After adding 0.45 wt% Er to Al–10%Mg_2Si–3.5%Cu alloy, Er-containing Al_8Cu_4Er phase appeared.

Figure 3 presents the optical micrographs of Al–10%Mg_2Si alloys without and with Er or/and Cu additions. It can be seen that all the microstructures of the Al–10%Mg_2Si alloys are composed of gray (α–Al+Mg_2Si) eutectic matrix and white primary α-Al dendrite distributed on the matrix, and black eutectic Mg_2Si particles are included in the eutectic matrix, which are a typical hypoeutectic structure. The primary α-Al dendrite was precipitated first from the melt during solidification and surrounded by subsequently solidified lamellar structure of the a binary eutectic α–Al+Mg_2Si.[2,3] In addition, a very small amount of black primary Mg_2Si particles appeared in the microstructure of the alloys, which is

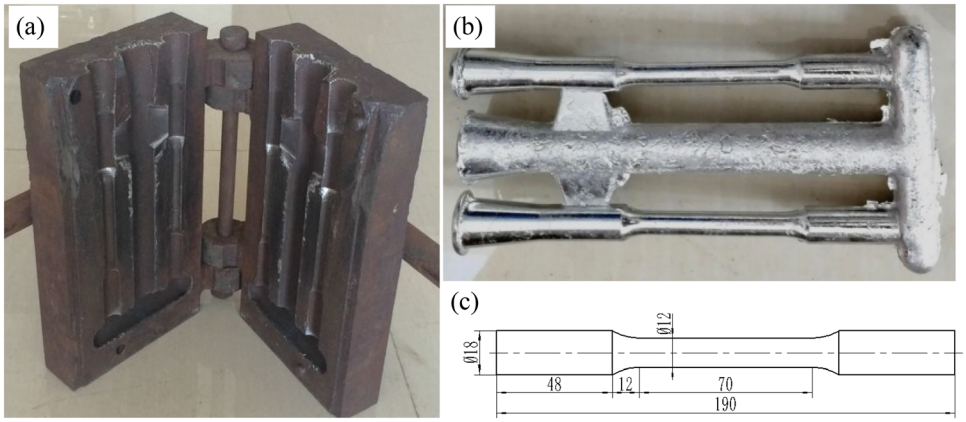

Figure 1. The permanent steel mould (a) and the castings+gating system for the cast tensile rod (b), and the dimensions of tensile specimen (c).

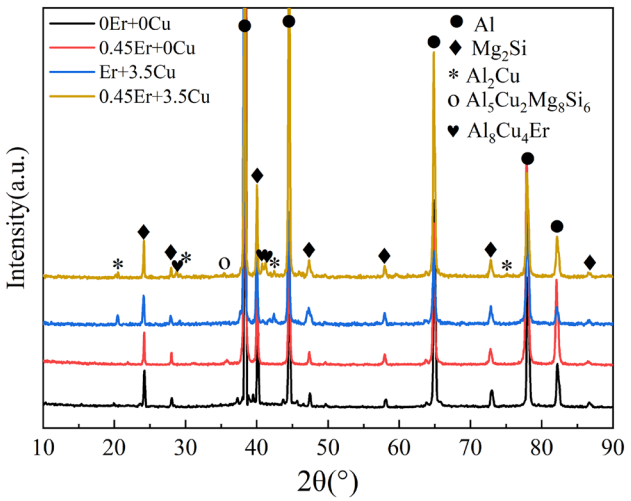

Figure 2. The XRD patterns of the experimental cast alloys.

consistent with the observation results in reference.[18] The occurrence of this phenomenon may be due to solute redistribution formed by non-equilibrium solidification in the cast-state, which causes segregation of Mg and Si atoms, leading to early precipitation of primary Mg_2Si particles before the alloy undergoes eutectic reaction.[18,19] Furthermore, the crystals of eutectic Mg_2Si in the alloy without Er and Cu additions exhibits a coarse Chinese character morphology (Fig. 3a), and the average length (L_M) and length to diameter ratio (L/B_M) of eutectic Mg_2Si crystals are as high as 15.7 μm and 25.6, respectively. After adding 0.45 wt% Er, the morphology and size of eutectic Mg_2Si crystals had undergone significant changes, the values of the L_M and L/B_M of eutectic Mg_2Si sharply declined, reached the minimum values of 4.2 μm and 7.8, respectively, and its morphology transformed from Chinese characters to fine particles and thin strips, as shown in Fig. 3b. When 3.5 wt% Cu was added separately, only a small portion of the eutectic Mg_2Si crystals changed into granules or dots, while others still presented a Chinese character-like morphology, and the size was slightly reduced (Fig. 3c). After adding 0.45 wt% Er to the alloy containing 3.5 wt% Cu, most of eutectic Mg_2Si crystals transformed into particles and thin strips, and the values of the L_M and L/B_M decreased to 5.7 μm and 9.1, respectively, as shown in Fig. 3d. These results indicate that the addition of Er in hypoeutectic Al–10%Mg_2Si alloys without and with 3.5 wt% Cu additions has a significant modification and refinement effect on eutectic Mg_2Si crystals. The average size (L_M) and length to diameter ratio (L/B_M) of eutectic Mg_2Si phase in the studied as-cast alloys are shown in Fig. 4.

In order to further discriminate the morphology of eutectic Mg_2Si, a 20% NaOH solution for deep corrosion treatment of the alloys was selected to corrode the primary and eutectic α-Al phase in the alloys and the three-dimensional morphology of eutectic Mg_2Si phase can be clearly observed, as shown in Fig. 5. The 3D morphology of eutectic Mg_2Si of the alloy without Er and Cu is characterized by thick, layered and plate-like structures (Fig. 5a). When 0.45 wt% Er was added to the Al–10%Mg_2Si alloy, the 3D morphology of the eutectic Mg_2Si was changed from a coarse layered structure to a fine coral-like and fibrous structure with more branches and irregular orientation, and its size significantly decreased, as shown in Fig. 5b. This indicates that the addition of Er transforms the growth of eutectic Mg_2Si into dendritic growth. After adding 3.5 wt% Cu to the alloy separately, the eutectic Mg_2Si remained in a layered and plate-like shape, but their length and thickness were smaller than those of the sample without Er and Cu (Fig. 5c). With adding 0.45 wt%Er and 3.5 wt% Cu together to the alloy, the morphology of the eutectic Mg_2Si was transformed into coral-like, as shown in Fig. 5d.

Figures 6, 7, 8 and 9 show the backscattered electron (BSE) micrographs, corresponding elemental spectra, and energy dispersive X-ray spectroscopy (EDS) analysis results of the studied as-cast alloys, respectively, to identify the category, size, morphology, and distribution of the second phase in the alloys except for Mg_2Si phase. It can be seen that many white phases with various shapes accumulated at the dendrite boundaries, boundaries between the dendrites and

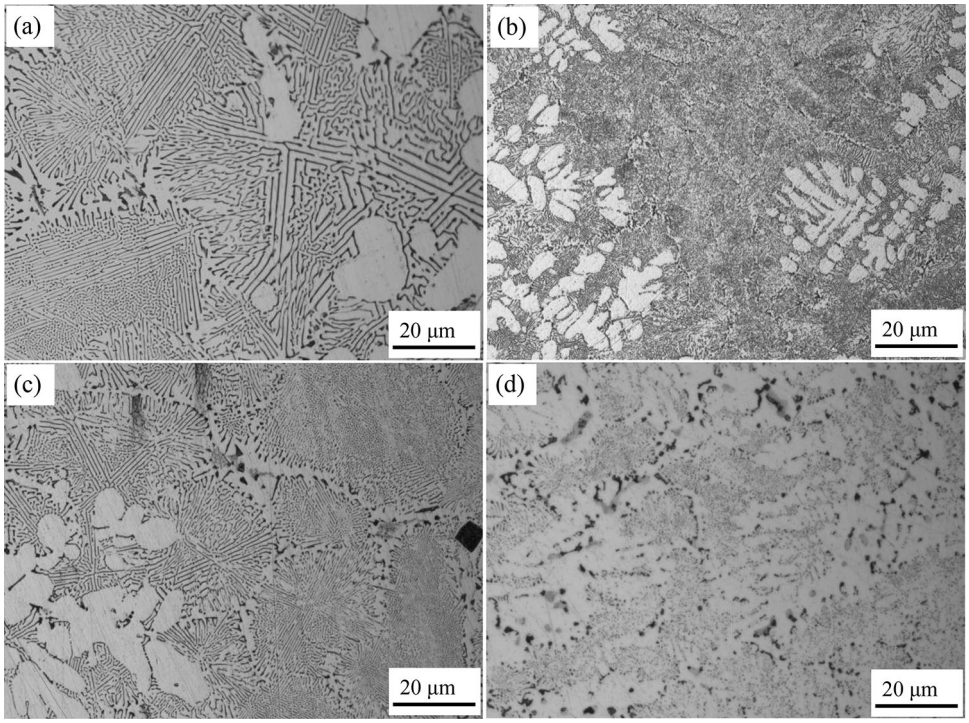

Figure 3. Optical microscopy (OM) images of studied alloys: (a) Al–10Mg_2Si, (b) 0.45Er, (c) 3.5Cu and (d) 0.45Er+3.5Cu.

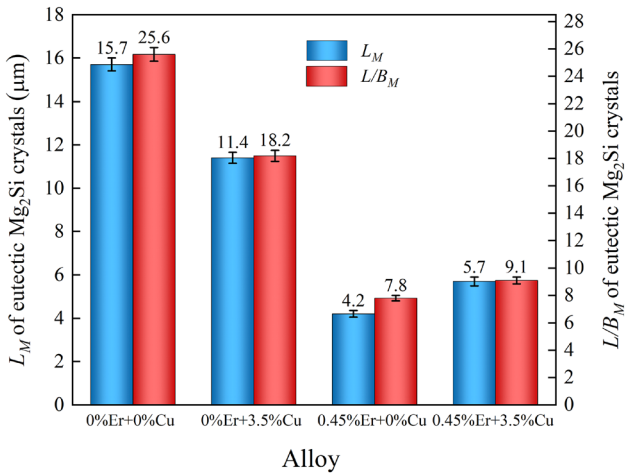

Figure 4. Average size (L_{Mg_2Si}) and length to diameter ratio (L/B_M) of eutectic Mg_2Si phase in the experimental cast alloys.

eutectic cells, and the boundary of eutectic cells (Fig. 6). For the alloy without the addition of Er and Cu, some needle-like phases were observed, which extended from the edge of α-Al dendrites towards the eutectic zone, and passed through the coarse plate-like eutectic Mg_2Si phase (Fig. 6a). EDS analysis indicates that the needle-like phase is β-Al_5FeSi (Fig. 9a), which has also been reported earlier in similar alloy.[20] After the addition of Er, Cu alone and Er + Cu together, the β-Al_5FeSi phase disappeared and was replaced by white and light gray phases with various morphologies. Only a small amount of small particles could be observed between eutectic cells in the alloy with the addition of Er (Fig. 6b), which was identified as Al_3Er phase (Fig. 9b). But after adding 3.5 wt% Cu, a large number of skeletal and bulk white phases appeared between Al/Mg_2Si eutectic cells and at the boundaries between eutectic cell and other eutectic cell (Fig. 6c). The elemental spectrum (Fig. 7) shows the enrichment of Al and Cu elements in this phase, accompanied by the presence of a small amount of Fe and Mg. High concentrations of Cu (26.64 at%) (Fig.9c) indicates that the phase is Al_2Cu, while a small amount of Fe (1.04 at%) and Mg (2.23 at%) elements were dissolved in it. In addition, irregular strip-like Al–Mg–Si–Cu quaternary phases enriched with Si (15.22 at%), Mg (7.69 at%) and Cu (1.28 at%) between eutectic cells could also be observed (Fig.6c) and detected (Fig. 9d). After adding 0.45 wt% Er to the alloy containing 3.5 wt% Cu, there was a significant change in the structure of the second phase. The coarse skeletal and bulk Al_2Cu phase was replaced by the phase with a fine feather-like, strip-like morphology, and evenly distributed along the edge of eutectic cell, as shown in Fig. 6d. Elemental spectra (Fig. 8) indicates that the phase is enriched with Al, Cu, and Er elements, EDS analysis further confirm that the phase is Al_8Cu_4Er phase containing Er (Fig. 9e). In addition, the Al–10%Mg_2Si–3.5%Cu–0.45%Er alloy also contains a small amount of Al–Mg–Si–Cu–Er pentagonal phase (Fig. 9f). It is interesting that the Er-containing phase precipitated in Al–10%Mg_2Si–3.5%Cu alloy with 0.45 wt% Er addition was identified as Al_8Cu_4Er phase, rather than Al_3Er phase precipitated in

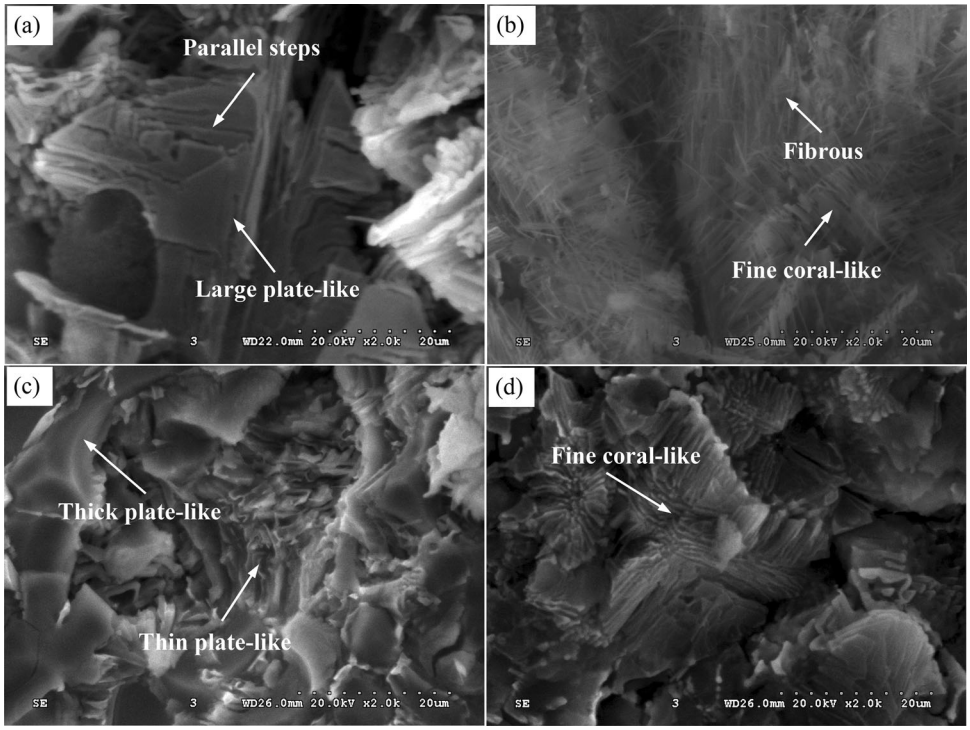

Figure 5. Scanning electron microscopy images of the three-dimensional eutectic Mg_2Si of the deep etched experimental alloys: (a) Al–10Mg_2Si, (b) 0.45Er, (c) 3.5Cu and (d) 0.45Er+3.5Cu.

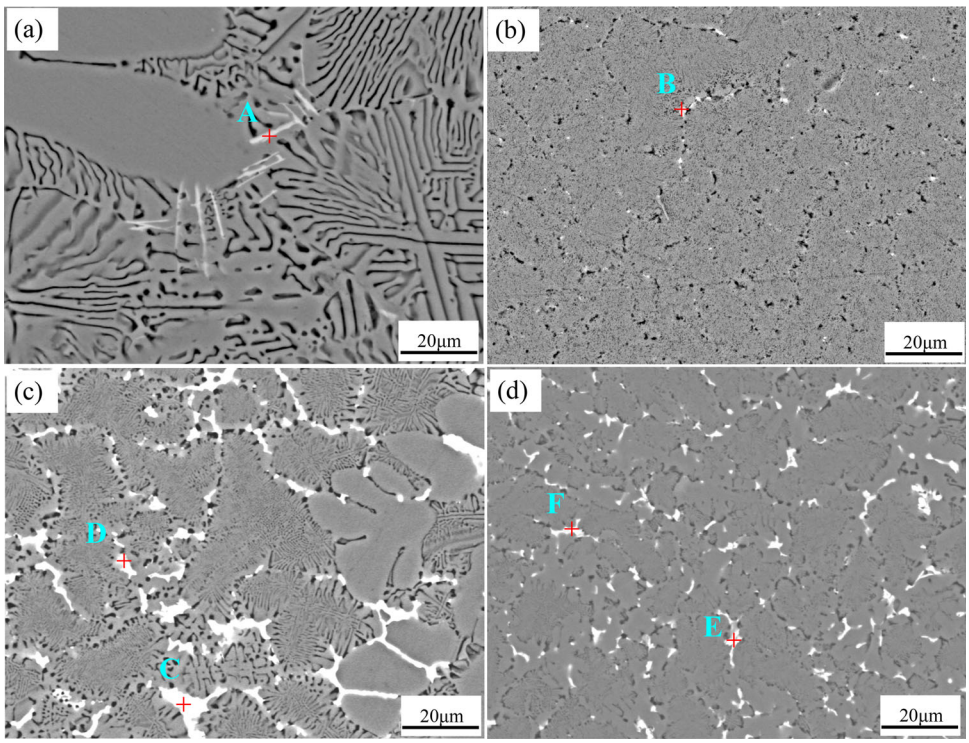

Figure 6. Backscattered electron (BSE) image of the experimental alloys: (a) Al–10Mg_2Si, (b) 0.45Er, (c) 3.5Cu and (d) 0.45Er+3.5Cu.

Al–Si or Al–Si–Mg alloy without Cu. Emamy et al. research[12] indicates that when the Cu content is high, the second phase is mainly Al_2Cu. In addition, It was also confirmed that the addition of Er in Al–Cu–Mg–Ag and Al–Zn–Mg–Cu alloys containing Cu element also led to the formation of Al_8Cu_4Er phase.[13,14]

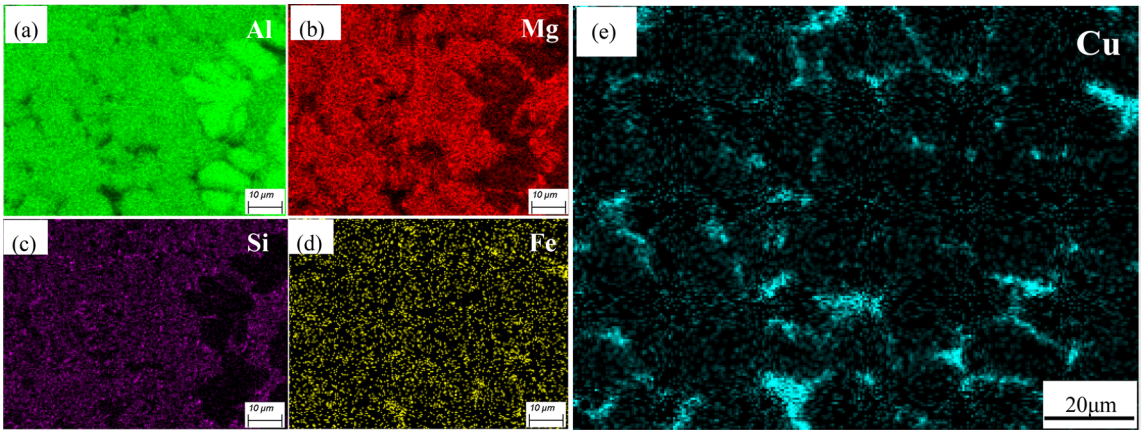

Figure 7. The corresponding element spectrum in Fig.5(c).

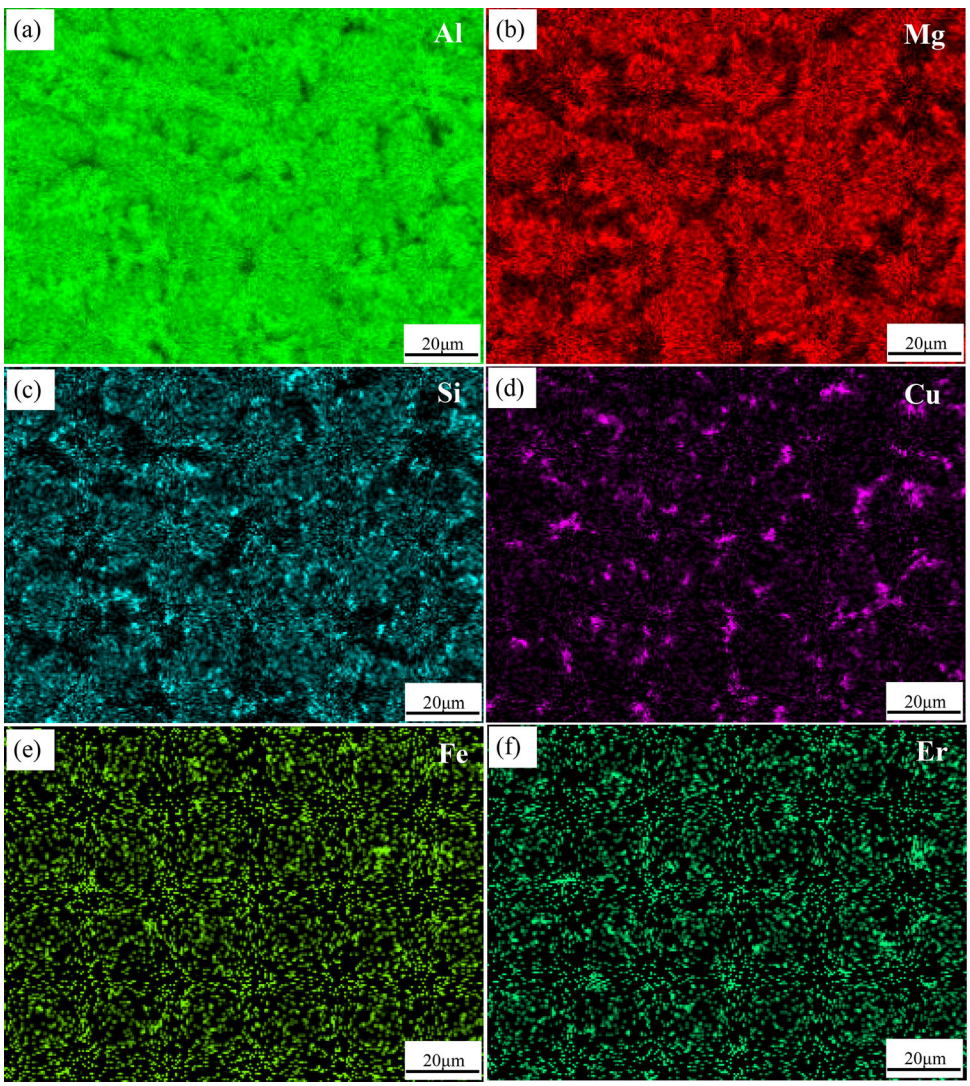

Figure 8. The corresponding element spectrum in Fig. 5(d).

Solid Solution Condition

Figure 10 shows the backscattered electron (BSE) micrograph of the studied alloy after solid solution treatment.

For Al–10Mg_2Si alloy, as shown in Fig. 10a, after solid solution treatment, the coarse and large layered eutectic Mg_2Si phase in the as-cast state completely disappeared, with some broken and spheroidized, while the other part

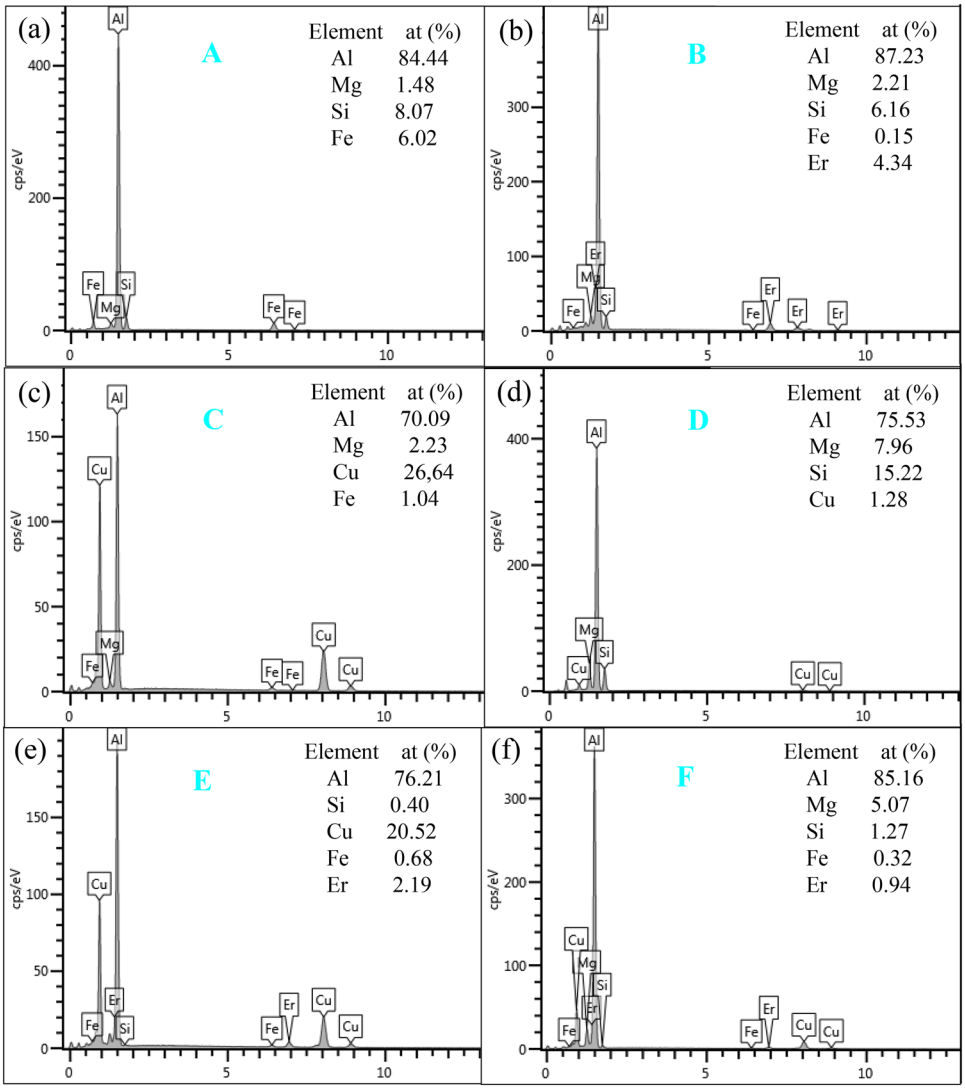

Figure 9. The corresponding EDS analysis of each point in Fig. 5.

still retained the long strip and sheet-like structure in the as-cast state, and some grains were still in the crushing stage. The average size (L_M) and length to diameter ratio (L/B_M) of the eutectic Mg_2Si phase decreased from 15.7 μm and 25.6 to 4.7 μm and 3.3, respectively, compared to those in the as-cast state. However, after the addition of Er alone, the eutectic Mg_2Si in the alloy was completely spheroidized, and the spherical particles were small and uniform in size. Only some Mg_2Si particles had a slightly larger diameter at the edge of the original eutectic cells (Fig. 10b), and L_M and L/B_M were reduced to 1.8 μm and 1.3, respectively, compared to those in the cast state. Although the majority of eutectic Mg_2Si phases with 3.5 wt% Cu added alone were transformed into spherical shapes, their spherical diameters were large and varied (Fig. 10c), with L_M and L/B_M being 3.6 μm and 2.5, respectively. After adding 0.45 wt% Er to the alloy containing 3.5 wt.% Cu, the eutectic Mg_2Si particles were also completely spheroidized, and the uniformity of the spherical diameter was greatly improved and was equivalent to that of alloy with the addition of Er alone (Fig. 10d), indicating that the addition of Er accelerates the fragmentation and spheroidization process of eutectic Mg_2Si phase during solid solution treatment, which is consistent with the results in reference.[15]The average size (L_M) and length to diameter ratio (L/B_M) of eutectic Mg_2Si phase in the studied alloys after solid solution treatment are shown in Fig. 11.

Figure 10 also shows the changes in intermetallic compounds in the studied alloys after solid solution treatment. After solid solution treatment, the number of intermetallic compounds in all studied alloys significantly decreased. For the alloy without the addition of Er and Cu, some elongated needle-like phases still existed around eutectic Mg_2Si particles (Fig. 10a). The corresponding element distribution is shown in Fig. 12a, indicating the enrichment of Al, Si, and Fe elements in the needle-like phase. EDS analysis was performed on point I above it (Fig. 13a), and the results showed that the phase was β–Al_5FeSi. The

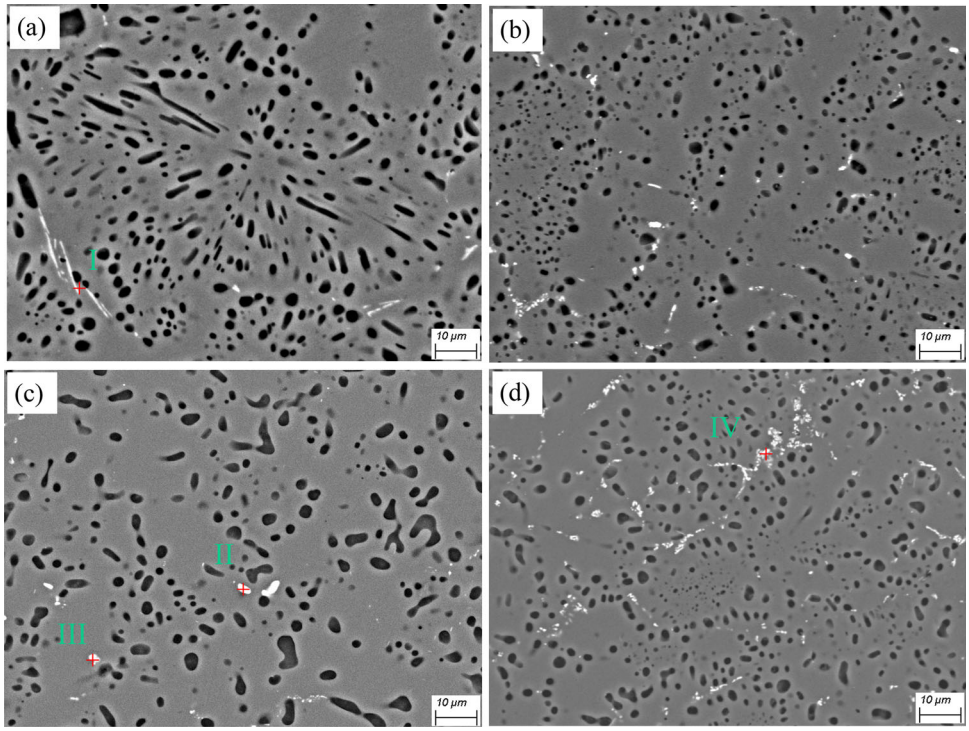

Figure 10. Backscattered electron (BSE) image of the experimental alloys after solid solution: (a) Al–10Mg$_2$Si, (b) 0.45Er, (c) 3.5Cu and (d) 0.45Er+3.5Cu.

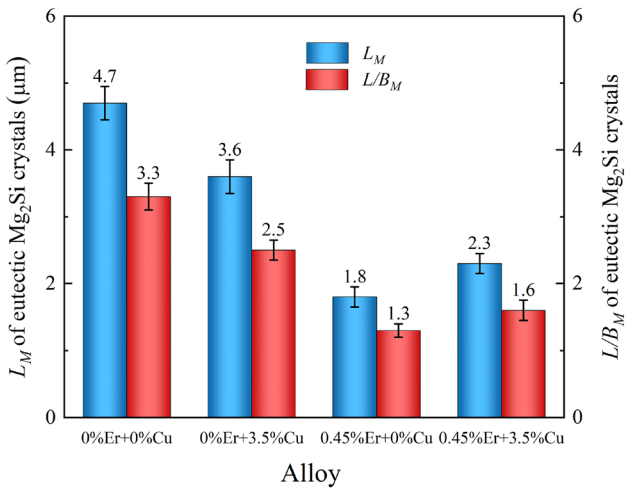

Figure 11. Average size (LMg$_2$Si) and length to diameter ratio (L/B$_M$) of eutectic Mg$_2$Si phase in the experimental alloys after solid solution.

morphology and size of the phase are not significantly different from those in the as-cast state, indicating that solid solution treatment cannot dissolve this phase in the matrix. The majority of intermetallic compounds in the alloys with Er or Cu added separately were solidly dissolved in the matrix, with only a few remaining. The difference is that the the size of residual particles added with Er are small (Fig. 10b), while the particles added with Cu are larger (Fig. 10c). These particles include Al_2Cu phase (Fig. 13b) and Al–Mg–Si–Cu quaternary phase (Fig. 13c), both of which contain high concentrations of Fe.

Compared with the aforementioned alloys, the alloy with the addition of Er and Cu resulted in more undissolved phases, which are distributed in the form of fine particles at the edges of the original eutectic cells, but its volume fraction is greatly reduced compared to the as cast state, as shown in Fig. 10d. Element distribution (Fig. 12b) and EDS analysis (Fig. 13d) indicate that these small particles enriched with Al, Cu, and Er elements, and they were confirmed to be an Al_8Cu_4Er phase with a small amount of Fe element. These results indicate that after 500×8 h solution treatment, the β-Al_5FeSi phase with the melting points higher than the solid solution temperature (500 °C) in Al–10%Mg_2Si alloy was undissolved and retained its needle-like morphology in as cast, while the $AlCu_2$ binary phase with low melting point in the studied alloy was solidly dissolved in the matrix. It is worth noting that the melting point of Al_8Cu_4Er phase is 575 °C,[14] which is higher than the solid solution temperature. The reason for its partial dissolution may be due to the decrease in melting point caused by the dissolution of Mg and Si atoms into the phase.

Tensile Properties

Figures 14 and 15 shows the typical stress-strain curve and the tensile properties including ultimate tensile strength

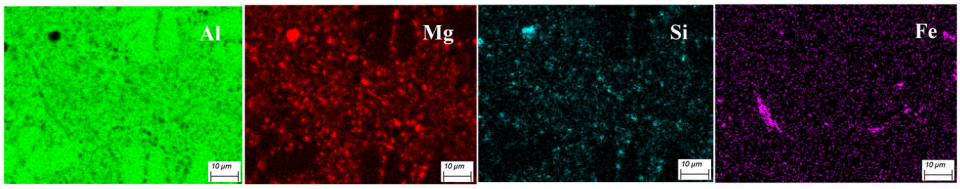

(a)

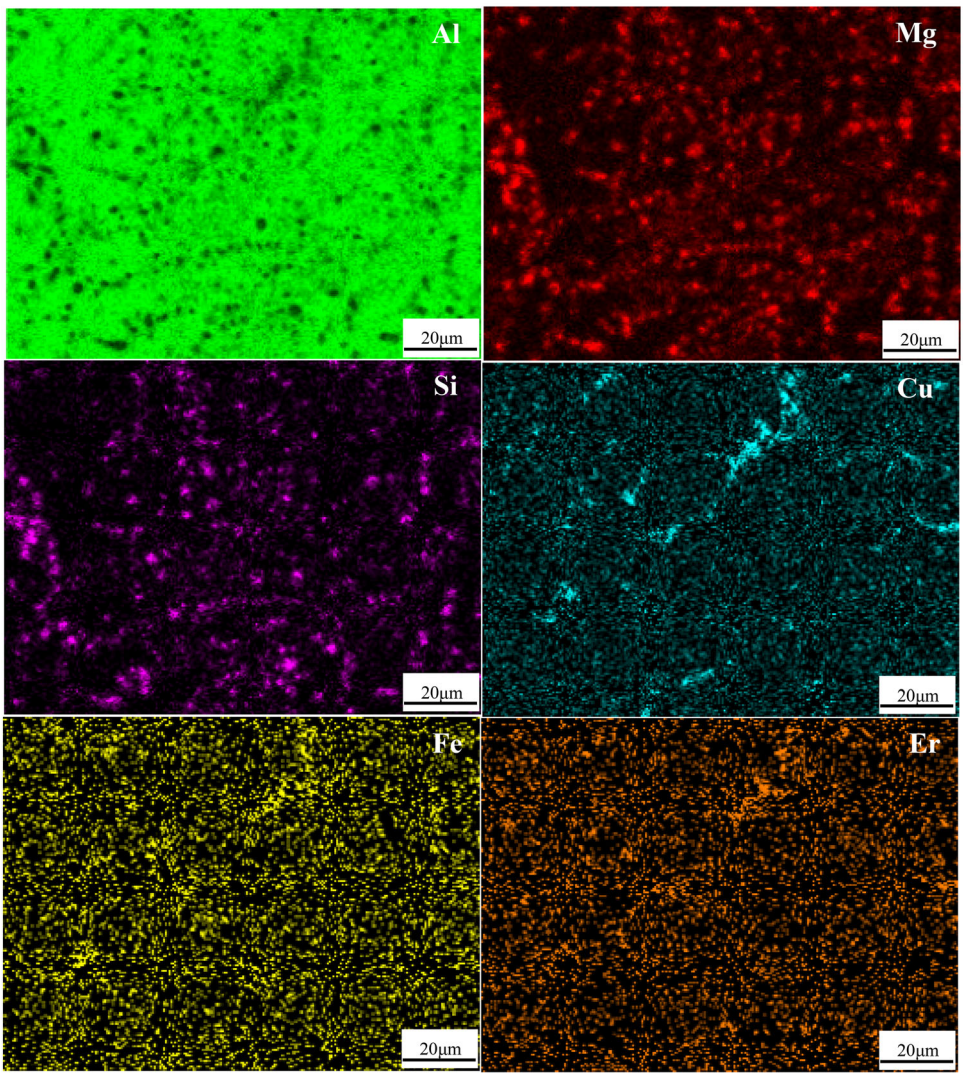

(b)

Figure 12. The corresponding element spectrum: (a) in Fig. 10(a) and (b) in Fig. 10(d).

(UTS), yield strength (YS), and elongation (EL)of the experimental alloys in the as-cast and T6 state. In Fig. 15, the error bars of six tensile specimens were marked at the top of each column reflecting the UTS, YS, and EL values of the experimental alloys at the as-cast and after solution aging. The error values of UTS, YS, and EL at the as-cast state are within the range of 3～5.2 MPa, 2～3 MPa, 0.05～0.2%, respectively, while the error values after solution aging are within the range of 3～5.5 MPa, 2～3 MPa, 0.05～0.4%, respectively. From Fig. 14a and 15a, it can be seen that the UTS, YS, and EL values of the cast tensile specimens without adding Er and Cu are 223.5 MPa, 114.9 MPa, and 2.1%, respectively. Adding 0.45 wt% Er increases the UTS, YS, and EL to 310.2 MPa, 133.4 MPa, and 4.9%, respectively. After adding 3.5 wt% Cu, the UTS and YS values increased, while EL sharply decrease to 1.3%. Adding Er to Al–10%Mg_2Si alloys without and with the addition of Cu simultaneously improved the tensile properties, and the UTS, YS, and EL values reached 356.1 MPa, 210.6 MPa, and 3.3%, respectively. After T6 treatment, the UTS values of the tensile specimens without the addition of Er and Cu, and with the

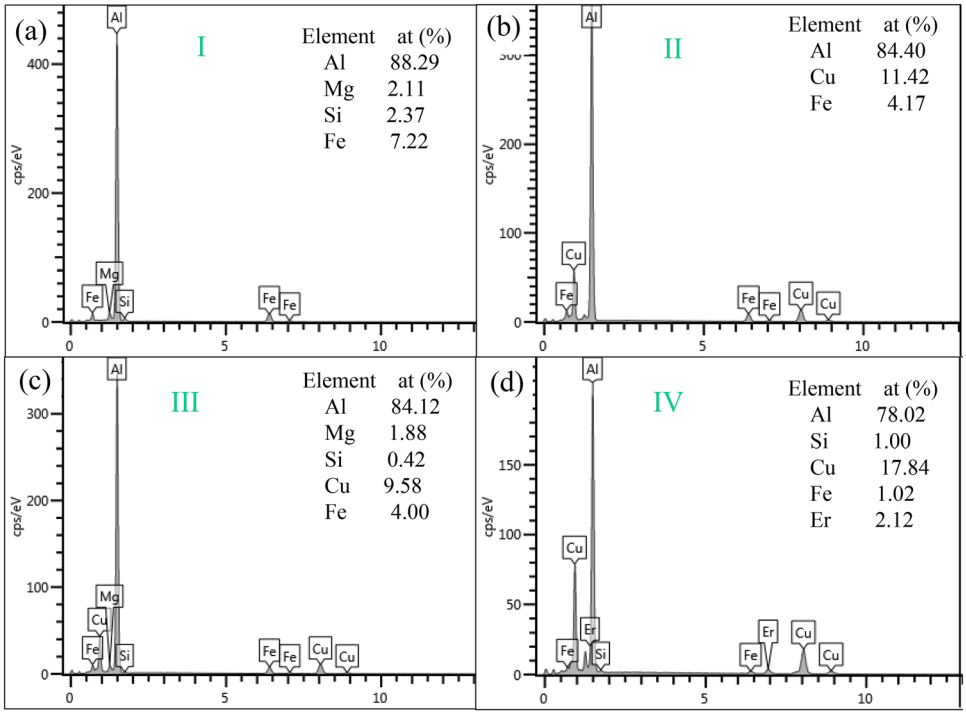

Figure 13. The corresponding EDS analysis of each point in Fig. 10.

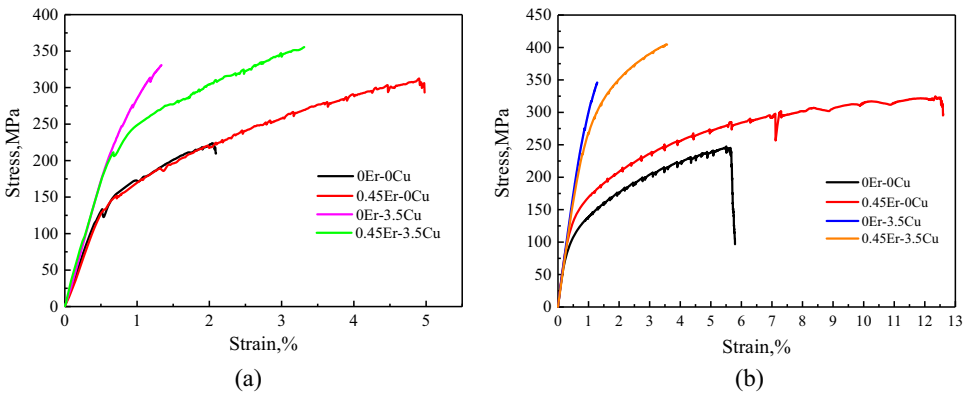

Figure 14. The typical stress-strain curve of the experimental alloys: (a) in the as-cast state and (b) after solid solution.

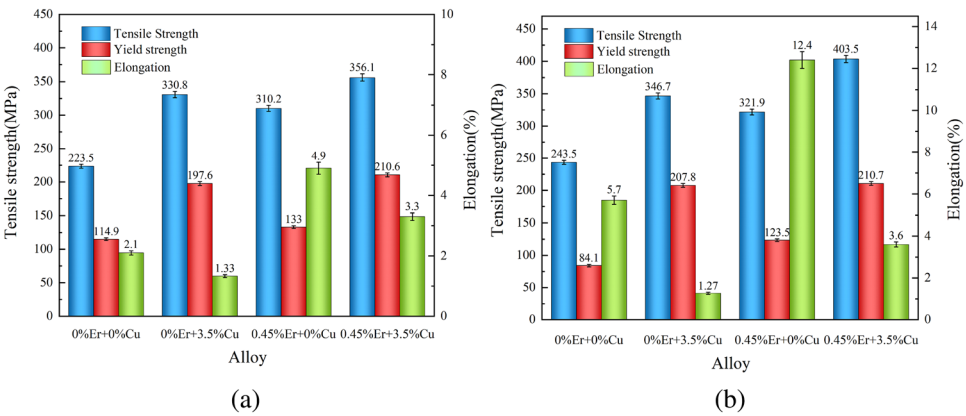

Figure 15. The UTS, YS, and EL values of the experimental alloys: (a) in the as-cast state and (b) after solid solution.

addition of Er alone slightly increased compared with the as-cast state, while the EL values increased significantly, especially the latter, increasing from 4.9 to 12.4%, respectively. While the EL values of the samples of Al–10%Mg_2Si–3.5%Cu alloys without and with Er addition do not change obviously, but the UTS values increased significantly, especially that of the alloy with the addition of Er, from 356.1 to 403.5 MPa (Figs. 14b and 15b).

Fractography

Figure 16 presents the SEM images of the fracture surface of the as-cast tensile specimen of the studied alloys.

As shown in Fig. 16a, the fracture surface of the tensile specimen without the addition of Er and Cu consisted of large irregular cleavage planes of coarse eutectic Mg_2Si and tearing ridges, and the cleavage planes with different directions were separated by the tearing ridges, indicating that the alloy exhibits quasi-cleavage and brittle fracture characteristics under tensile action. After adding 0.45 wt% Er, the irregular cleavage planes on the fracture surface of the samples disappeared, and a large number of small and deep dimples covered the entire cross-section, as shown in Fig. 16b, indicating that the fracture of the alloy transformed into ductile fracture mode. With the addition of 3.5 wt%Cu, the fracture surface of the tensile specimen mainly composed of irregular cleavage planes, but their sizes decreased, and a small amount of dimples were observed (Fig. 16c), showing mixed quasi cleavage and dimple morphology. When 0.45 wt% Er was added to the Cu-containing alloy, a large number of dimples reappeared, also showing the characteristics of ductile fracture, as shown in Fig. 16d. Interestingly, upon careful observation of the figure, it was found that small black eutectic Mg_2Si blocks at the bottom of most of the dimples were encapsulated by the eutectic α-Al matrix and deeply trapped within it.

Figure 17 shows the tensile fracture surface of the the studied alloys after T6 heat treatment. After T6 heat treatment, some ductile dimples appeared on the fracture surfaces of Al–10%Mg_2Si and Al–10%Mg_2Si–3.5%Cu alloys without the addition of Er, but a large number of irregular cleavage planes and long cracks were still retained (Fig. 17a and c). In the Al–10%Mg_2Si and Al–10%Mg_2Si–3.5%Cu alloys with the addition of Er, small and deep dimples covered the entire fracture surface, which is a typical ductile fracture feature (Fig. 17b and d).

Discussion

Refinement and Modification of Eutectic Mg_2Si

The morphology and grain size of eutectic phases in aluminum alloys are closely related to its nucleation and growth mode during the solidification process.[21] It is well known that the commercial-purity aluminum ingots used in

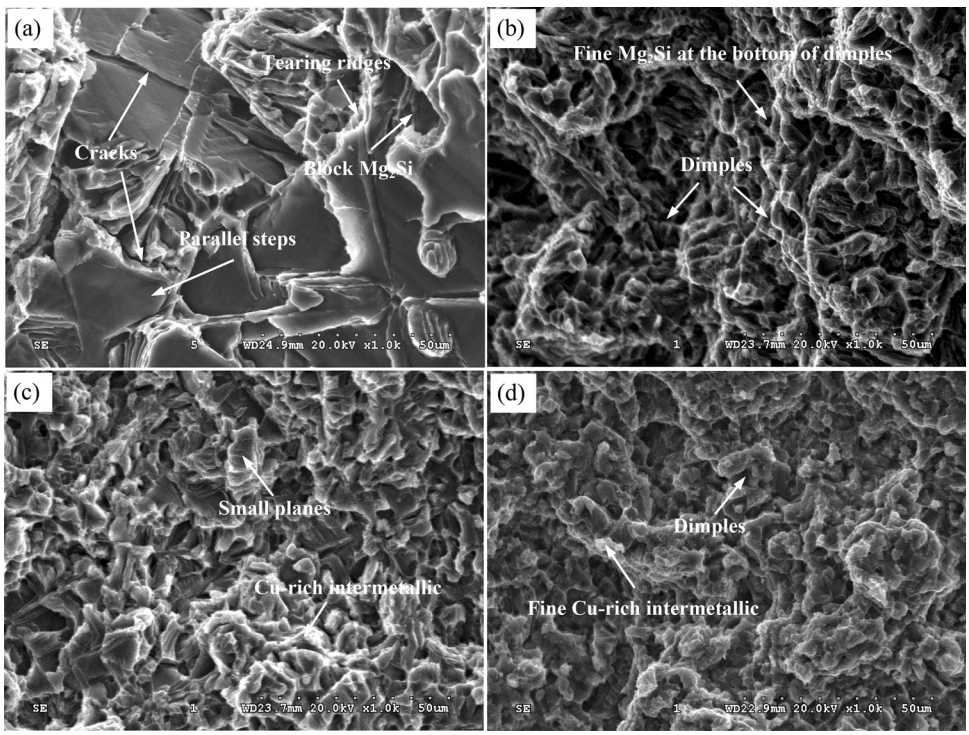

Figure 16. Scanning electron microscopy images of tensile fracture of the experimental cast alloys: (a) Al–10Mg_2Si, (b) 0.45Er, (c) 3.5Cu and (d) 0.45Er+3.5Cu.

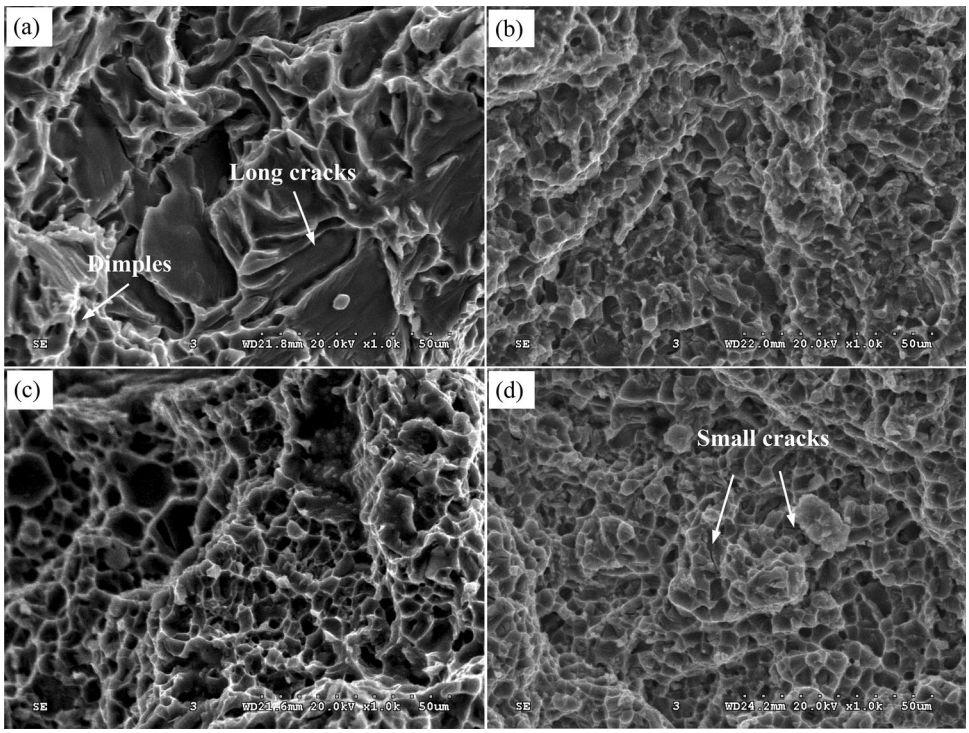

Figure 17. Scanning electron microscopy images of tensile fracture of the experimental alloys after T6: (a) Al–10Mg_2Si, (b) 0.45Er, (c) 3.5Cu and (d) 0.45Er+3.5Cu.

aluminum foundry alloys always contain residual trace impurity P element. Before the precipitation of eutectic phase, P reacts with liquid Al to form AlP phase, which has an important impact on the formation of eutectic phase in the alloys. According to the suppression nucleation theory, one phase can act as heterogeneous nucleating site for the other phase when there is a good coherent relationship existing on the interface of two types of phase.[22] Therefore, the interatomic distance of the crystal face of the two phases should be close to each other, and the atomic arrangement of the crystal faces should be similar. AlP is a zinc-blende structure with lattice parameter: a=5.42 Å and Mg_2Si is a face centered cubic anti fluorite structure (CaF2) with lattice parameter: a=6.39 Å. Li et al.[23] calculated the disregistry between the (220) crystal plane of AlP and the (311) crystal plane of Mg_2Si by using the Turnbull-Vonnegut formula with a value of 6.58%. Sun et al.[24] investigated the interfacial properties of AlP/Mg_2Si interface by using first-principles calculations and the calculation results show that AlP(100)/Mg_2Si(211) and AlP(331)/Mg_2Si(110) interfaces can form steadily. These results indicate that the Mg_2Si has a good lattice matching coherence relationship with AlP, and AlP phase is an excellent heterogeneous nucleation point for Mg_2Si phase and can heterogeneous nucleating site for Mg_2Si. Li et al.[23] also found the presence of AlP particles in the core of Mg_2Si phase through electron probe microanalysis (EPMA).

Therefore, when the temperature of the aluminum liquid drops to the eutectic temperature, due to the presence of AlP phase in the aluminum liquid, eutectic Mg_2Si is easily nucleated on its surface, which greatly increases the nucleation temperature of eutectic Mg_2Si and correspondingly reduces the undercooling of the Al–Mg_2Si eutectic reaction. The free growth of eutectic Mg_2Si does not require high undercooling, so it grows into thick Chinese character-like morphology at very low undercooling. After adding modification elements to the alloy, the modifying elements will preferentially combine with the P element in the alloy to form a P-containing phase with a crystal structure different from that of Mg_2Si phase, inhibiting the formation of AlP phase in the alloy.[23] The SEM (Fig. 18a) and EDS results (Fig. 18b) clearly indicate that Cu and Er reacted with impurity P to form Er–P–Cu compounds instead of AlP, which depletes the more effective heteronuclear AlP particles in the melt, forcing eutectic Mg_2Si to nucleate at higher undercooling and form fine structures.

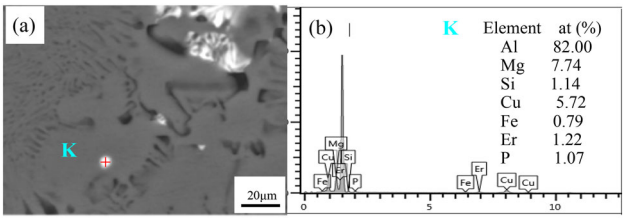

Figure 18. Backscattered electron (BSE) image of a particle within the α-Al grain (a) and EDS analysis at K point (b).

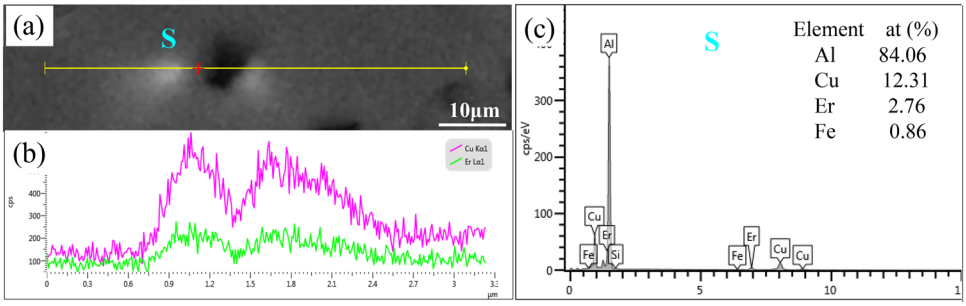

Figure 19. Backscattered electron (BSE) image around a eutectic Mg_2Si particle (a), the line scan (b) and EDS analysis at S point (c).

On the other hand, the growth mode of eutectic Mg_2Si phase also has a significant impact on its final morphology and grain size,[25,26] and the change in the morphology of eutectic Mg_2Si phase is the results of competitive growth between α-Al and eutectic Mg_2Si phase.[27] In the case of Al–10%Mg_2Si alloy, the eutectic Mg_2Si phase grows faster and forms plate-like and Chinese character-like structures compared to eutectic α-Al phase. For Al–10%Mg_2Si without and with Cu alloys containing 0.45 wt% Er, when the temperature drops to the eutectic point, Er atoms are repelled into the liquid between the generated eutectic phases by the primary and eutectic α-Al particles due to low Er in the primary and eutectic α-Al phases, enrich in the liquid phase at the eutectic interface and form undercooling at the front of the liquid-solid growth interface, which inhibits the growth of the eutectic Mg_2Si phase and reduces its growth rate, resulting in a finer crystal morphology. Therefore, it may be inferred that the enrichment of Er atoms at the liquid/solid growth interface result in a decrease in the average crystal size (L_M) and aspect ratio (L/B_M) of the eutectic Mg_2Si phase (Fig. 4), as well as a transformation of its morphology from the shape of Chinese characters to that of thin strips and fibers (Figs. 3 and 5). The distribution of Er element around the eutectic Mg_2Si phase with the addition of Er were analyzed through element area scan by SEM and EDS, as shown in Fig. 19. Some light white shadows were seen around an eutectic Mg_2Si particle (Fig. 19a), and the surface scanning image (Fig. 19b) indicates the enrichment of Er and Cu in these shadows. According to the results of EDS analysis (Fig. 19c), the Er contents at the S point on the edge of the eutectic Mg_2Si is as high as 2.76 at.%, indicating the presence of enrichment of Er.

Improvement of Mechanical Mroperties

The above experimental results indicate that the addition of Er and solution treatment simultaneously improve the strength and plasticity of the Al–10%Mg_2Si alloys without and with the addition of Cu, which is attributed to the refinement and modification of Er and solution treatment on eutectic Mg_2Si and intermetallic compounds phases.

Improvement of Strength

The studied alloys are composed of a soft α-Al matrix, and hard eutectic Mg_2Si or/and intermetallic compounds. The strength of a material mainly depends on its ability to delay dislocation movement.[28] The hard eutectic Mg_2Si and intermetallic compound particles in the alloys, as second phase particles, can effectively hinder the movement of existing and form dislocations during the stretching process. The moving dislocations bypass the non-deformable these particles and form dislocation rings around them. During the deformation process, the number of dislocations increases exponentially, and the critical shear stress required for the dislocation line to continue moving increases, greatly improving the strength of the alloy. The strengthening efficiency of the second phase particles can be described as the Orowan formula:[29]

$$\sigma_{\text{Orown}} = \frac{Gb}{2\pi(1-\nu)} \cdot \frac{1}{\lambda} \cdot \ln\left(\frac{D}{B}\right)$$

where σ_{orown} is the yield strength of the material, G is the shear modulus, b is the Boltzmann vector, ν is the Poisson's ratio, λ is the pitch of the second phase, and D is the average size of the second phase. Eq. indicates that the strength of an alloy is inversely proportional to the average size of the second phase and directly proportional to the number of second phases. That is, the smaller the size of the second phase and the more its number, the higher the strength of the alloy. The addition of 0.45 wt%Er to Al–10%Mg_2Si alloys without and with the addition of 3.5%Cu decreases the value of L_M of eutectic Mg_2Si from 15.7 μm (without Cu) and 11.4 μm (with Cu) to 5.7 μm, respectively (Fig. 4), and the grain size of Cu-containing intermetallic also is decreased obviously (Figs. 6, 7, 8), leading to the increase in the value UTS of the alloy from 223.5 MP (without Cu) and 330.8 MP (with Cu) to 356.1 MPa respectively, as shown in Fig. 15a.

The main reason why solid solution treatment significantly improves the strength of the alloy is the strengthening effect of fine, dispersed nanoscale precipitates on the alloy. The precipitation of nanoscale particles after solid solution aging exhibits a coherent relationship with α-Al matrix, is

firmly bound, and distributed evenly and dispersedly. When these particles meet the dislocations generated within the α-Al crystal under external force, they neither crack nor detach from the matrix, which creates a strong blocking effect on the movement of dislocations, causing the dislocation lines to bend. As the curvature of dislocation lines increases, dislocation loops are formed around the particles. The smaller and more particles there are, the greater the resistance to dislocation movement, and the stronger its strengthening effect on the alloy. Extensive research has shown that aluminum alloys containing trace amounts of Er, after solid solution-aging or homogenization treatment, precipitate not only the main strengthening phase but also the L12-structured trialuminide nano Al_3Er dispersoids coherent with α-Al matrix. The nano Al_3Er is a promising precipitate that can enhance precipitation and inhibit recrystallization.[30] The fine secondary Al_3Er particles precipitated by supersaturation strongly hinder the movement of dislocations and increase the shear stress required for dislocation sliding.[31] In addition, the Al_3Er dispersoids precipitated first in Al–3%Cu[32] and Al–4%Cu–1.3%Mg[33] alloys with trace amounts of Er can serve as the heterogeneous nucleation core of Cu-containing nano θ', refined θ' phase, further strengthening α-Al matrix. It is inferred that after T6 treatment, the tensile strength of Al–10%Mg_2Si–3.5%Cu–0.45%Er alloy with the addition of Er and Cu, reaching up to 403.5 MPa (Fig. 15b), could be due to the dispersed strengthening of Cu-containing nano θ' and Al_3Er dispersoids. Further research is needed to investigate the effect of Er's microalloying on Al–10%Mg_2Si–3.5%Cu alloys.

Improvement of Plasticity

The fracture mode and plasticity of aluminum alloys reinforced by a hard second phase is closely related to the morphology of the second phase.[34,35] When the alloy is subjected to tensile load, the soft α-Al matrix is first subjected to force, gradually transmitted to the interface between the matrix and the second phase, and then the second phase itself. The behavior of the second phase during the stretching process includes the detachment of the second phase from the Al matrix and its own fracture.[36] The detachment of the second phase depends on the interface strength between the second phase and α-Al matrix.[37] The morphology of the second phase is an important factor affecting the interface strength. The more irregular the morphology, the more uneven the stress distribution at the interface, which is more likely to cause the detachment of the second phase at the interface.

For the Al–10%Mg_2Si–(3.5%Cu) alloys without Er addition, the brittle fracture and low plasticity of the alloys are caused by the debonding and rapid crack propagation of eutectic Mg_2Si and Cu-containing phases during early stretching. Due to the fact that the phases in the alloys are a coarse Chinese character-like eutectic Mg_2Si, and the needle-like phase β-Al_5FeSi phase without Cu and the irregular bulk Cu-containing intermetallic compounds (with Cu), which are easy to cause stress concentration at their tips, becoming a source of cracks under external loads, resulting in the debonding of eutectic Mg_2Si and irregular bulk Cu-containing intermetallic compounds at the interface before the load is transferred to them, especially those that are approximately perpendicular to the tensile direction had already been debonded and small cracks at the interface formed. The interfaces of other coarse eutectic Mg_2Si in eutectic region provided an easy path for crack propagation and the fracture path gone preferentially through these eutectic regions.[38] Thus, under the continuous action of the load, the cracks rapidly expanded along primary α-Al and the eutectic Mg_2Si boundaries, and connected, forming a fracture surface characterized by large irregular cleavage planes and tearing ridges (Fig. 16a and c), and some coarse long cracks at the interface between the eutectic Mg_2Si and the Al matrix, and a fractured needle-like β-Al_5FeSi phase were seen on the surfaces near the side views of fractured alloy samples, as shown in Fig. 20a, leading to brittle fracture mode and low low plasticity. In the case of Al–10%Mg_2Si–3.5%Cu–0.45%Er alloy containing the eutectic Mg_2Si with fine strip-like morphology, the tensile force can be transferred from the Al matrix to the the interface due to the more uniform stress distribution at the interface during the tensile process, which hinders the growth of dislocations in the Al matrix at the interface front, resulting in a significant increase in dislocation density. At the same time, voids will be generated at the Mg_2Si particles. These voids grow as the Al matrix undergoes further strain, and ultimately coalesce through an internal necking mechanism, forming ductile fracture surface features of dimples. The presence of a large number of dimples, accompanied by small Mg_2Si particles encapsulated inside on the fracture surfaces (Fig. 16d), and some parallel thin strips observed near the fracture surface near the side views, as shown in Fig. 20c, indicate that the alloy had produced a large amount of plastic deformation in the Al matrix before fracture, which is confirmed in the simultaneous improvement of elongation and strength at the macro level (Fig. 15a).

The significant improvement in plasticity for all studied alloys after T6 heat treatment (Fig. 15b), especially Al–10%Mg_2Si–0.45%Er alloy, is mainly due to the morphology transformation of eutectic Mg_2Si from Chinese character-like in the as cast state into spherical shape after solid solution treatment (Fig. 10), which further reduces the stress concentration at the interface between the eutectic Mg_2Si and α-Al matrix. A large number of parallel thin strips in a large area away from the side view fracture surface presented and some dislocation slip bands obstructed in front of small eutectic Mg_2Si particles for the Al–10%Mg_2Si–0.45%Er alloy after heat treatment (Fig. 20d) confirmed that the alloy undergone significant

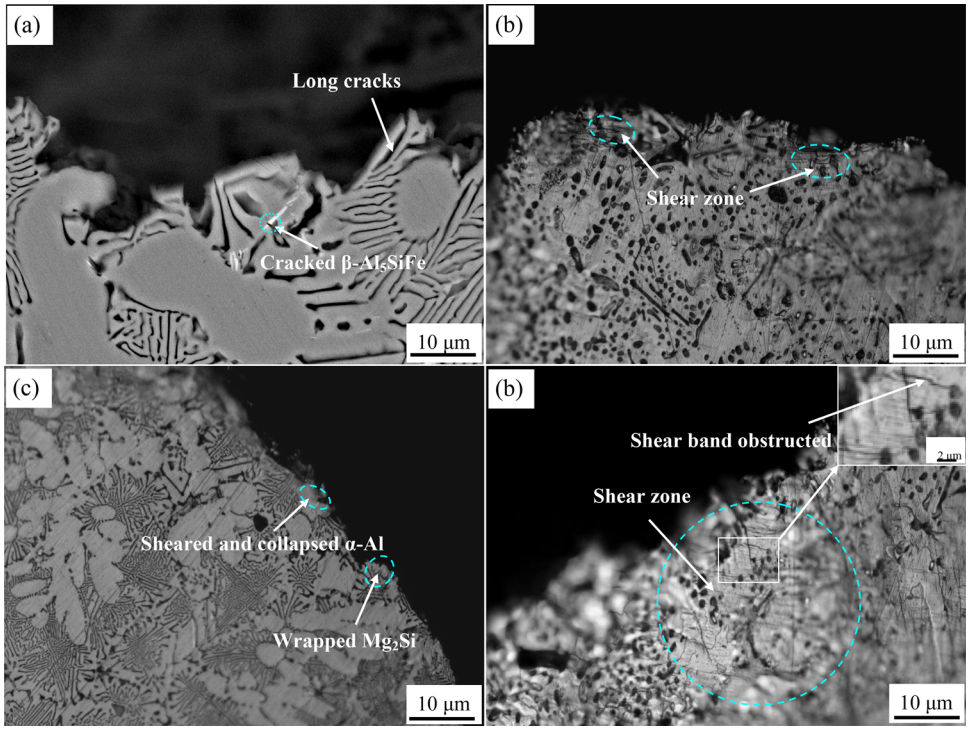

Figure 20. Optical microscopy (OM) images of the surfaces near the side views of tensile fractured alloys: (a) cast Al–10Mg_2Si alloy, (b) Al–10Mg_2Si alloy after T6, (c) Al–10Mg_2Si–3.5Cu–0.45Er cast alloy and (d) Al–10Mg_2Si–0.45Er alloy after T6.

plastic deformation before tensile fracture, resulting in an EL value of up to 12.4% after solution treatment. It is worth noting that after T6 treatment, a large amount of dispersed phases precipitated in the microstructure of Er and Cu samples, effectively strengthening the Al matrix and greatly improving the strength (Fig. 10). However, according to the solid solution aging mechanism,[39] it inevitably leads to a decrease in plasticity value. In fact, compared with that in the as-cast state, its EL value did not decrease and instead slight increase, from 3.3% in as-cast state to 3.6% in T6, which is the result of eutectic Mg_2Si spheroidization.

Conclusion

In the present work, the effects of Er addition and solution treatment on the microstructure, tensile properties and fracture behavior of Al-10%Mg_2Si-(3.5%Cu) alloy have been investigated systematically. From the experimental results obtained, the following conclusions are:

1. The addition of 0.45 wt% Er to hypoeutectic Al–10%Mg_2Si alloy without and with the addition of 3.5 wt% Cu can significantly reduce the grain sizes of eutectic Mg_2Si phase, and transform the morphology of the eutectic Mg_2Si from coarse Chinese characters to thin stripes, dots, and fibers. The modification of eutectic Mg_2Si is attributed to the inhibition of Er on the heterogeneous nucleation of AlP by forming Er, P-containing phases, and the enrichment of Er atoms around the eutectic Mg_2Si phase, which inhibits the growth of eutectic Mg_2Si and promotes a change in its growth direction. The growth of eutectic grains is constrained by the distribution of Er and the undercooling of the corresponding components before grain boundaries.
2. Needle-like Fe-containing phase β-Al_5FeSi in Al–10%Mg_2Si alloy after adding Er or (and) Cu disappears, while small, discontinuous Al_8Cu_4Er phase in the Al–10Mg_2Si–3.5Cu alloy containing Er precipitate along the edge of eutectic cells, replacing the coarse, blocky Al_2Cu phase in the Cu alloy containing only Cu.
3. The solid solution treatment causes the eutectic Mg_2Si to tend towards spheroidization, which is promoted by the addition of Er. During the solid solution period, the fragmentation and spheroidization of eutectic Mg_2Si grains in alloys with the addition of Er are fine and globalized. Additionally, after 500 °C × 8 h solid solution treatment, the phases without Fe and Er in studied cast alloys are completely dissolved, while the Fe-containing phase is completely retained for needle-shaped β-Al_5FeSi phase in Al–10%Mg_2Si and partially retained for Al_8Cu_4Er phase in Al–10%Mg_2Si–3.5%Cu-0.45%Er alloy.

4. The addition of 0.45 wt% Er simultaneously improves the strength and plasticity of the cast alloys without and with the addition of 3.5 wt% Cu. The YS, UTS, and EL of the cast alloy with the addition of Er and Cu together displayed the highest values of 345 MPa, 280 MPa, and 7.1%, respectively. The solid solution treatment further improved the tensile properties of the studied alloys, especially the plasticity of Al–10%Mg_2Si alloy containing Er and the tensile strength of Al–10%Mg_2Si–3.5%Cu alloy containing Er were significantly increased, reaching 12% and 408 MPa, respectively. The improvement of strength of the alloy after as-cast and T6 treatment is due to the obstruction of fine eutectic Mg_2Si and containing-Er/Cu intermetallic compound particles on dislocations, while the improvement of plasticity mainly lies in the reduction of stress concentration and stress uniformity around eutectic Mg_2Si and intermetallic compounds caused by the regularity and spheroidization of eutectic Mg_2Si phase morphology.
5. The brittleness of Al–10%Mg_2Si alloys without and with the addition of 3.5 wt% Cu comes from the decohesion of coarse eutectic Mg_2Si particles in the early stage of stretching, while the large amount of plastic deformation generated before cracking of fine eutectic Mg_2Si particles is responsible for the high ductility of the Al–10%Mg_2Si–(3.5%Cu) alloys with the addition of Er.

Acknowledgements

This work was supported by the National Natural Science Foundation of China (NSFC) (Grant Nos. 51971106), the Education Department of Jiangxi Province (Grant No. GJJ2202921, GJJ2202905), the Liaoning Natural Science Foundation of China (Grant No. 2019-MS-171), and the Programs for Liaoning Innovative Talents and Liaoning Distinguished Professor.

REFERENCES

1. F. Yan, Development of high strength Al–Mg_2Si–Mg based alloy for high pressure diecasting process. Brunel University. PhD thesis (2013)
2. S. Ji, D. Watson, Z. Fan, M. White, Development of a super ductile diecast Al–Mg–Si alloy. Mater. Sci. Eng. A **556**, 824–833 (2012)
3. J. Zhang, Z. Fan, Y.Q. Wang, B.L. Zhou, Equilibrium pseudobinary Al–Mg_2Si phase diagram. Mater. Sci. Technol. **17**, 494–496 (2001)
4. X.F. Wu, K.Y. Wang, R.D. Zhao, F.F. Wu, Enhanced mechanical properties of hypoeutectic Al–10Mg_2Si cast alloys by Bi addition. J. Alloys Compd. **767**, 163–172 (2018)
5. W.Q. Jiang, X.F. Xu, Y.G. Zhao, Z. Wang, C. Wu, D. Pan, Z.Y. Meng, Effect of the addition of Sr modifier in different conditions on microstructure and mechanicalproperties of T6 treated Al–Mg_2Si in-situ composite. Mater. Sci. Eng. A **721**, 263–273 (2018)
6. R. Du, D. Yuan, F. Li, D.C. Zhang, S.S. Wu, S.L. Lü, Effect of in-situ TiB_2 particles on microstructure and mechanical properties of Mg_2Si/Al composites. J. Alloys Compd. **776**, 536–542 (2019)
7. C. Li, C. Wang, P.K. Ma, J. Xu, Z.Z. Yang, M. Zha, J.G. Wang, H.Y. Wang, Effect of Sb modification on microstructure and mechanical properties of hypoeutectic Al–11Mg_2Si alloy. Mater. Sci. Eng. A **782**, 1–16 (2020)
8. X.W. Hu, F.G. Jiang, F.R. Ai, H. Yan, Effects of rare earth Er additions on microstructure development and mechanical properties of die-cast ADC12 aluminum alloy. J. Alloys Compd. **538**, 21–27 (2012)
9. M. Colombo, E. Gariboldi, A. Morri, Er addition to Al–Si–Mg-based casting alloy: effects on microstructure, room and high temperature mechanical properties. J. Alloys Compd. **708**, 1234–1244 (2017)
10. P. Pandee, U. Patakham, C. Limmaneevichitr, Microstructural evolution and mechanical properties of Al–7Si–0.3Mg alloys with erbium additions. J. Alloys Compd. **728**, 844–853 (2017)
11. G.K. Sigworth, Fundamentals of solidification in aluminum castings. Int. J. Metals Cast. **8**, 7–20 (2014)
12. M. Emamy, N. Nemati, A. Heidarzadeh, The influence of Cu rich intermetallic phases on the microstructure, hardness and tensile properties of Al–15%Mg_2Si composite. Mater. Sci. Eng. A **527**, 2998–3004 (2010)
13. Y.T. Li, Z.Y. Liu, Q.K. Xia, Y.B. Liu, Grain refinement of the Al–Cu–Mg–Ag alloy with Er and Sc additions. Metall. Mater. Trans. A **38**, 2853–2861 (2007)
14. Y.C. Huang, C.C. Zhang, X.W. Ren, Y. Liu, S.Z. Chen, Y.L. Wang, Existence form of trace Er in Al–Zn–Mg–Cu alloy and its Genetic Effect. Rare Metal Mat. Eng. **48**, 2848–2856 (2019)
15. W.R. Osório, L.R. Garcia, P.R. Goulart, A. Garcia, Effects of eutectic modification and T4 heat treatment on mechanical properties and corrosion resistance of an Al–9 wt% Si casting alloy. Mater. Chem. Phys. **106**(2–3), 343–349 (2007)
16. Y. Jin, H. Fang, S. Wang, R. Chen, Y. Su, J. Guo, Effects of Eu modification and heat treatment on microstructure and mechanical properties of hypereutectic Al–Mg_2Si composites. Mater. Sci. Eng. A **831**, 142227 (2022)
17. Z.D. Li, C. Li, Y.C. Liu, L.M. Yu, Q.Y. Guo, H.J. Li, Effect of heat treatment on microstructure and mechanical property of Al–10%Mg_2Si alloy. J. Alloys Compd. **663**, 16–19 (2016)

18. P. Biswas, M.K. Mondal, H. Roy, D. Mandal, Microstructural evolution and hardness property of *in situ* Al–Mg_2Si composites using one-step gravity casting method. Can. Metall. Q. **56**(3), 340–348 (2017)
19. S.R. Wang, R. Ma, Y.Z. Wang, Y. Wang, L.Y. Yang, Growth mechanism of primary silicon in cast hypoeutectic Al−Si alloys. Trans. Nonferrous Met. Soc. China **22**, 1264–1269 (2012)
20. J.C. Chenc, M.X. Li, Z.Y. Yu, Z.Y. Meng, C. Wang, Z.Z. Yang, H.Y. Wang, Simultaneous refinement of α-Mg grains and β-$Mg_{17}Al_{12}$ in Mg-Al based alloys via heterogeneous nucleation on Al8Mn4Sm. J. Magnes. Alloy **11**, 348–360 (2023)
21. J.H. Li, M. Albu, F. Hofer, P. Schumacher, Solute adsorption and entrapment during eutectic Si growth. Acta Mater. **83**, 187–202 (2015)
22. J.M. Rigsbee, H.I. Aaronson, A computer modeling study of partially coherent fcc: bcc boundaries. Acta Metall. Mater. **27**, 351–363 (1979)
23. C. Li, X.F. Liu, Y.Y. Wu, Refinement and modification performance of Al–P master alloy on primary Mg_2Si in Al–Mg–Si alloys. J. Alloys Compd. **465**, 145–150 (2008)
24. J.Y. Sun, C. Li, X.F. Liu, L.M. Yu, H.J. Li, Y.C. Liu, Investigation on AlP as the heterogeneous nucleus of Mg_2Si in Al–Mg_2Si alloys by experimental observation and first-principles calculation. Results Phys. **8**, 146–152 (2018)
25. H.C. Shin, J.Y. Son, B.K. Min, Y.S. Choi, K.M. Cho, D.H. Cho, I.M. Park, The effect of Ce on the modification of Mg_2Si phases of as-cast eutectic Mg-Si alloys. J. Alloys Compd. **792**, 59–68 (2019)
26. C. Li, Y.Y. Wu, H. Li, X.F. Liu, Morphological evolution and growth mechanism of primary Mg_2Si phase in Al–Mg_2Si alloys. Acta Mater. **59**, 1058–1067 (2011)
27. T.Y. Liu, X. Zou, C. Yang, Y. Pan, Y.Y. Ren, Y.M. Li, Investigation on morphology of primary Mg_2Si in Al–20 wt%Mg2Si composite with experiment and first-principle calculations. Mater Charact **187**, 111836 (2022)
28. A.M.A. Mohamed, F.H. Samuel, Influence of Mg and solution heat treatment on the occurrence of incipient melting in Al–Si–Cu–Mg cast alloys. Mater. Sci. Eng. A **543**, 22–34 (2012)
29. F.L. Wang, J.J. Bhattacharyya, S.R. Agnew, Effect of precipitate shape and orientation on Orowan strengthening of non-basal slip modes in hexagonal crystals application to magnesium alloys. Mater. Sci. Eng. A **666**, 114–122 (2016)
30. G.F. Xu, S.Z. Mou, J.J. Yang, T.N. Jin, Z.R. Nie, Z.M. Yin, Effect of trace rare earth element Er on Al-Zn-Mg alloy. Trans. Nonferrous Met. Soc. China **16**, 598–603 (2006)
31. M. Shakoori Oskooie, H. Asgharzadeh, H.S. Kim, Microstructure, plastic deformation and strengthening mechanisms of an Al–Mg–Si alloy with a bimodal grain structure. J. Alloys Compd. **632**, 540–548 (2015)
32. S.W. Pan, X.H. Chen, X.L. Zhou, Z.D. Wang, K.X. Chen, Y.D. Cao, F. Lu, S.H. Li, Micro-alloying effect of Er and Zr on microstructural evolution and yield strength of Al–3Cu (wt%) binary alloys. Mater. Sci. Eng. A **790**, 139391 (2020)
33. C. Xu, Z.Y. Liu, S. Bai, Y. Li, L.H. Lin, Alloying behavior of erbium in an Al–Cu–Mg alloy. J. Alloys Compd. **505**, 201–205 (2010)
34. M.R. Ghorbani, M. Emamy, N. Nemati, Microstructural and mechanical characterization of Al–15%Mg_2Si composite containing chromium. Mater. Des. **32**, 4262–4269 (2011)
35. P. Biswas, D. Mandal, M.K. Mondal, Compressive failure analysis of in-situ Al–Mg_2Si composites: experiment and finite element modelling. Eng. Fract. Mech. **277**, 108986 (2023)
36. X. Zhang, J.Y. Hu, B.X. Dong, X. Li, S.Q. Kou, S. Zhang, F. Qiu, Effect of Cu and Zn elements on morphology of ceramic particles and interfacial bonding in TiB_2/Al composites. Ceram. Int. **48**, 25894–25904 (2022)
37. A. Weck, D.S. Wilkinson, E. Maire, Observation of void nucleation, growth and coalescence in a model metal matrix composite using X-ray tomography. Mater. Sci. Eng. A **488**, 435–445 (2008)
38. A. Razaghiana, A. Bahrami, M. Emamy, The influence of Li on the tensile properties of extruded in situ Al–15%Mg_2Si composite. Mater. Sci. Eng. A **532**, 346–353 (2012)
39. A. Zhu, B.M. Gable, G.J. Shiflet, E.A. Starke Jr., Trace element effects on precipitation in Al–Cu–Mg–(Ag, Si) alloys: a computational analysis. Acta Mater. **52**(12), 3671–3679 (2004)